# Biocatalytic Self-Assembly on Magnetic Nanoparticles

*Maria P. Conte,[a] Jugal Kishore Sahoo,[a, b] Yousef M. Abul-Haija,[a, c] K. H. Aaron Lau,[a,*] and Rein V. Ulijn[a, d, e, f, *]*

a. WestCHEM/Department of Pure & Applied Chemistry, University of Strathclyde, 99 George Street, Glasgow, G1 1RD, U.K.; E-mail: aaron.lau@strath.ac.uk

b. Department of Chemical and Biomolecular Engineering, McCourtney Hall, University of Notre Dame, IN, 46556

c. WestCHEM/School of Chemistry, The University of Glasgow, Glasgow G12 8QQ, UK

d. Advanced Science Research Center (ASRC) of the Graduate Center, City University of New York, 85 St Nicholas Terrace, New York NY10027, United States; E-mail: rein.ulijn@asrc.cuny.edu

e. Department of Chemistry and Biochemistry, City University of New York – Hunter College, 695 Park Ave., New York, NY 10065, USA.

f. PhD Program in Chemistry, The Graduate Center of the City University of New York, New York, NY 10016, USA.

KEYWORDS Peptides, Self-Assembly, Enzymes, Enzyme immobilization, Biocatalysis, Magnetic Nanoparticles

ABSTRACT Combining (bio-)catalysis and molecular self-assembly provides an effective approach for the production and processing of self-assembled materials, by exploiting catalysis to direct the assembly kinetics and hence control the formation of ordered nanostructures. Applications of (bio-)catalytic self-assembly in biologically interfacing systems and in nanofabrication have recently been reported. Inspired by self-assembly in biological cells, efforts to confine catalysts on flat or patterned surfaces to exert spatial control over molecular gelator generation and nanostructure self-assembly have also emerged. Building on our previous work in the area, we demonstrate in this report the use of enzymes immobilized onto magnetic nanoparticles (NPs) to spatially localize the triggering of peptide self-assembly into nanofibers around NPs, in order to enable enhanced properties and magnetically responsive behavior in the resulting nanofibrous hydrogel. The concept is generalized for both an equilibrium biocatalytic system that forms stable hydrogels and a non-equilibrium system that normally has a preset lifetime. Characterization of the hydrogels shows that self-assembly occurs at the site of enzyme immobilization on the NPs, to give rise to gels with an "hub-and-spoke" morphology where the nanofibers are linked through the enzyme-NP conjugates. This NP-controlled arrangement of self-assembled nanofibers enables remarkable enhancements in the shear strength of both hydrogel systems, as well as a dramatic extension of the hydrogel stability in the non-equilibrium system. The use of magnetic NPs enables external control of both the formation of the hydrogel and its overall structure by application of an external magnetic field.

## 1. Introduction

The combination of (bio)catalysis and supramolecular self-assembly[1-5] provides a powerful means to direct supramolecular materials formation.[6-11] This approach is inspired by dynamic materials found in biological systems, where self-assembly is often coupled to, and regulated by, catalysis.[12-14] A number of enzymes have been utilized in biocatalytic self-assembly, including phosphatases, esterases and proteases.[12, 14-15] These catalysts are typically dissolved in self-assembly precursor solutions to enable catalytic formation of self-assembly building blocks and consequent structure generation over time.

The possibility to employ surface immobilized catalysts has also been investigated, in order to achieve spatial control over the locale of the self-assembly process. Williams *et al*. first employed immobilized thermolysin on an amine functionalized glass surface to enable localized self-assembly of Fmoc-protected peptides on a surface.[16] Vigier-Carriere *et al*. employed alkaline phosphatase, which was immobilized in a polyelectrolyte multilayer, to trigger the self-assembly and gelation of a Fmoc-protected tripeptide.[17] More recently, they employed a chymotrypsin adsorbed layer on a substrate to catalyze the condensation of short modified peptides into oligomers, which self-assemble into a fibrillar network at the interface.[18] Using non-enzymatic catalysts, Olive *et al*. employed patterned sulfonic acid groups to catalyze the local formation of supramolecular assemblies, leading to the formation of micropatterns of supramolecular structures.[13] In

addition, the Xu group has exploited localized biocatalytic assembly within living systems to influence the fate of cancer cells.[19-20]

It is clear that surface confined biocatalytic self-assembly holds promise both in biologically interfacing systems and as a tool in bottom-up nanofabrication.[16, 19-22] In fact, we recently highlighted the potential of selecting between gradually releasing or covalent immobilized enzymes on a surface to obtain either a self-assembled bulk hydrogel or a sub-nanometer thick surface network of nanofibers.[23] However, to our knowledge, there are no reports that specifically demonstrate localized biocatalytic nucleation and self-assembly of nanostructures from nanoparticle-immobilized enzymes. Moreover, we are not aware of reports where the locale of the immobilized enzymes could be externally controlled for nanostructure self-assembly.

In this study, we employed enzyme-magnetic nanoparticle (NP) conjugates for self-assembly initiation and post-assembly control of a hydrogel. We selected two biocatalytic self-assembly systems that we have been studying: an thermodynamic controlled system based on condensation-driven assembly by thermolysin (System 1),[24] and a kinetic system based on competing transacylation-driven assembly and hydrolytic disassembly catalyzed by chymotrypsin (System 2).[25] We followed the self-assembly process through a series of gelation experiments using reverse-phase high-performance liquid chromatography (RP-HPLC) measurements. We characterized the peptide nanostructures by transmission electron microscopy (TEM) and circular dichroism (CD) spectroscopy, and analyzed how the structural morphology influenced the mechanical strength of our gels, which was measured by oscillatory rheometry. Finally, we investigated the further consequences of

the spatial organization of the catalytic activity through manipulating the enzyme-NP conjugates with an externally applied magnetic field.

## 2. Results and Discussion

### 2.1. System Design and NP Preparation

System 1 is a thermodynamically controlled system that exploits thermolysin (from *Bacillus thermoproteolyticus*) for reversible enzymatic condensation of peptide precursors to form self-assembling gelators (Fig. 1b).[24] System 2 is a non-equilibrium, kinetically controlled system using chymotrypsin (from bovine pancreas) that has the potential to both generate self-assembly building blocks or break them down through competing acylation and hydrolysis reactions (Fig. 1b).[25]

Magnetic nanoparticles (NPs) were chosen to enable externally applied spatial control over the self-assembly process (*i.e.* stimuli-responsive behavior), without requiring chemical or direct mechanical manipulation of the NPs. We immobilized thermolysin and chymotrypsin on commercially available iron oxide NPs that have an average diameter of 500 nm. These NPs have a polyethylene glycol (PEG) coating terminated with carboxylic acid groups that we used for EDC/NHS coupling of the enzymes (see section 1 in ESI and Fig. 1a). We found that the NP size chosen allowed for easy separation of the nanoparticles with commercially available magnetic separation racks.

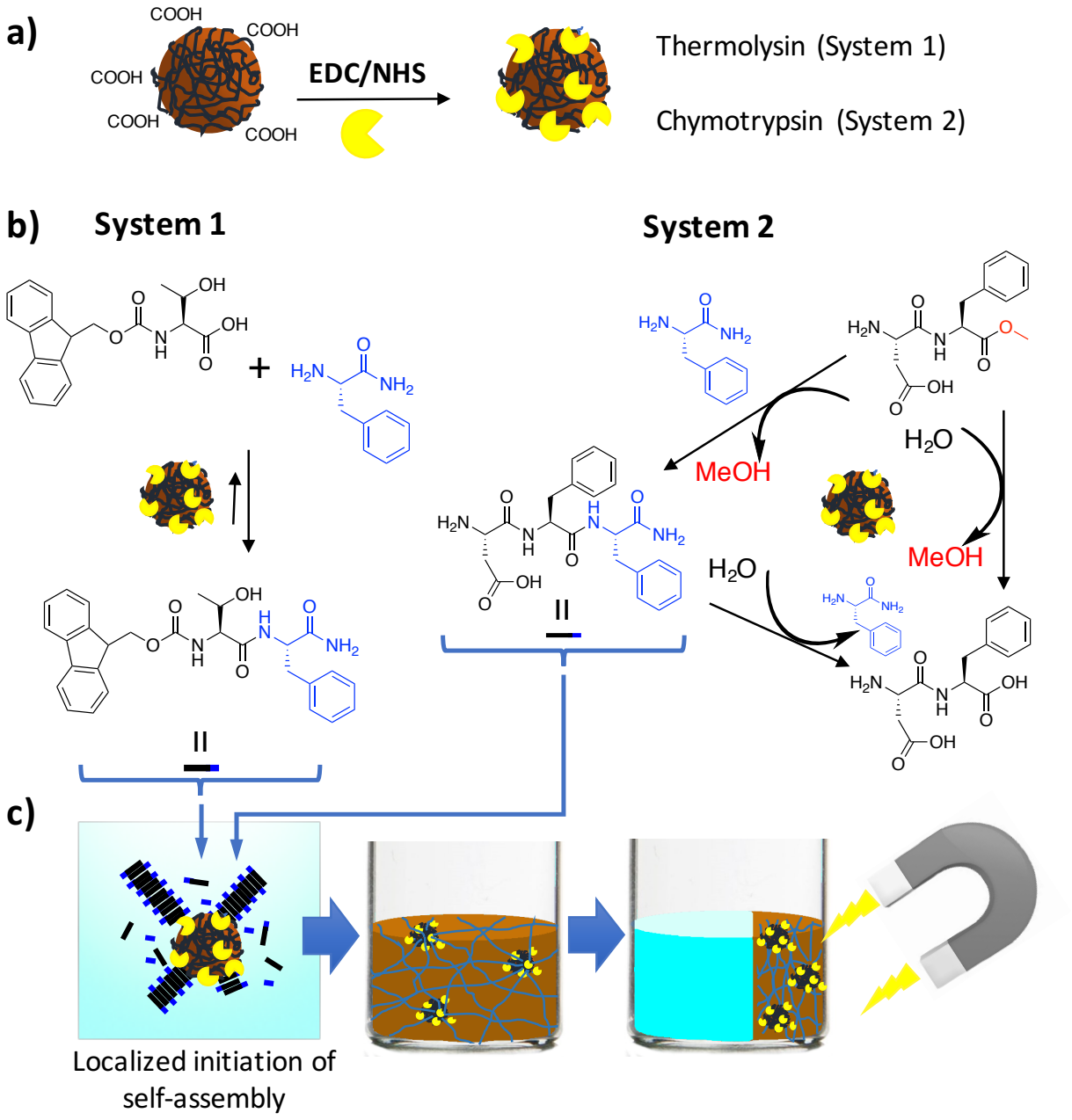


Figure 1 a) Schematic illustration of the enzyme immobilization on PEG-COOH modified nanoparticles by EDC/NHS coupling. b) Reaction of the precursors Fmoc-T and F-$NH_2$ with thermolysin-NP conjugates to give the gelator Fmoc-TF-$NH_2$ (System 1) and the precursors DF-OMe and F-$NH_2$ with chymotrypsin-NPs to give the gelator DFF-$NH_2$ (System 2). c) Schematics of the localized initiation of self-assembly onto the magnetic NPs and external manipulation of the formed hydrogel with a magnet.

Fluorescence spectroscopy was performed to monitor the activity of immobilized thermolysin and chymotrypsin *via* a previously reported and highly sensitive Förster resonance energy transfer (FRET) assay using a cleavable peptide sequence E(EDANS)-G-T/L-G-K(DABCYL) (where the T/L link indicates the cleavage site).[26] The nanoparticle-enzyme conjugates were washed multiple times to remove any weakly bound adsorbed enzymes. The FRET assay was first performed on the wash solutions (section 2 in ESI and Fig. S1a and S1c) to ensure complete removal of non-covalently bound enzymes. When activity was no longer detected, indicating that any loosely bound enzymes had been washed away, the FRET assay was performed on the nanoparticle-enzyme conjugates to characterize the immobilized enzyme activity. Significant immobilized activities were measured on both thermolysin and chymotrypsin conjugates (section 2 in ESI). The immobilized enzyme activity in both nanoparticle systems was approximately equivalent to 10 $\mu$g/ml of "free" enzymes dissolved in solution (see ESI section 2.1). The enzyme-NP conjugates were separated from the supernatant by means of a magnetic separation rack and collected for localized biocatalytic self-assembly experiments.

2.2.Gelation Behavior of Thermolysin System 1

Thermolysin-nanoparticle conjugates were added to a solution of the non-assembling precursors Fmoc-T (20 mM) and F-$NH_2$ (80 mM) in a glass vial. We have previously shown that thermolysin can catalyze amide bond formation between Fmoc-T and F-$NH_2$ to generate Fmoc-TF-$NH_2$, which then self-assembles into nanofibrous hydrogels.[24] In the present experiments, the thermolysin-NP and precursor mixture was briefly vortexed and

left to equilibrate. 20 µl samples of the mixture were taken at a series of time points for analysis by RP-HPLC to characterize the conversion of the precursors into Fmoc-TF-$NH_2$ self-assembling gelators.

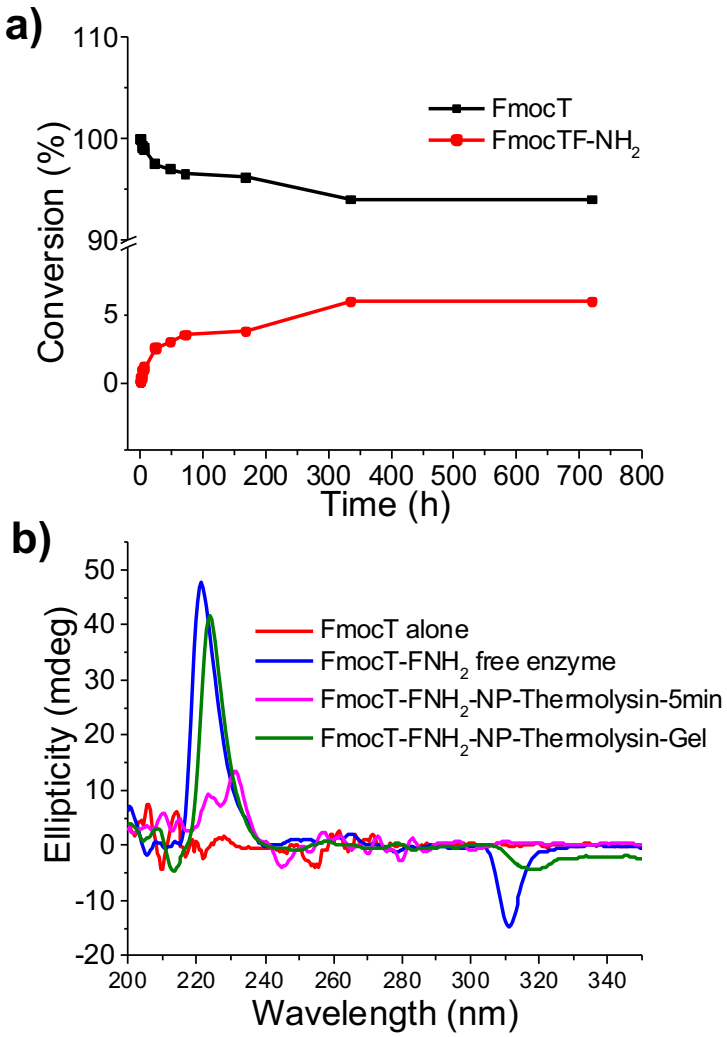


Figure 2: HPLC conversion (c) and CD spectra (d). The conversion of the precursors into the final products reaches almost 6% after approximately 12 days for System 1. The observed CD spectrum shows a positive signal around 220 nm, indicating the formation of chiral structures over time. The peak at 310 nm relates to chirally organized fluorenyl groups.

Fig. 2a shows that the conversion into Fmoc-TF-$NH_2$ slowly increased over time, reaching ca. 3.5% at 3 days and a plateau of 6% after 12 days. This apparently low conversion, corresponding to 0.58 mg/ml of peptide in the gel, was unexpected from

preliminary visual inspection, which showed the formation of a light brown clear gel (by the 4th day; Fig. 4a, inset). In comparison, in our previous study with surface-released thermolysin, a bulk gel was observed with a conversion yield of 30% and 2.9 mg/ml of gelators obtained by 4 days.[23] In earlier studies using free enzymes, a conversion yield of ca. 35% was usually observed after around 1h as a bulk gel is formed.[24]

Setting aside the ability to form a gel for the moment, the low conversion observed is reasonable considering the system conditions. First, the overall concentration of the enzyme is much lower compared to previous studies (see above).[23-24] In addition, as shown previously,[23] surface-immobilized thermolysin catalyzes the conversion into gelators and the subsequent self-assembly only in the vicinity of the immobilization surface. This spatial localization of the gelators is likely facilitated by the low solubility of the Fmoc-peptides formed. We observed that the NPs had gradually precipitated to the bottom of the vial over the multi-day experiment. Nonetheless, the fact that a bulk gel was formed in System 1 implies that the enzyme-NP conjugates were sufficiently dispersed throughout the bulk of the solution to enable nanofiber self-assembly without enzyme release.

The molecular organization of the self-assembled nanofibers in System 1 was first monitored with circular dichroism (CD) spectroscopy (Fig. 2b). The CD spectrum measured at the start of the experiment (CD measurement complete at t = 5 min) showed the appearance of a small positive peak around 220-230 nm. This peak grew in intensity upon gel formation, and it corresponds to the CD signature observed for gels formed with free enzyme, indicating the formation of chiral arrangements as previously reported.[27]

Secondly, TEM images of the gel material revealed a high density of nanofibers around the biocatalytic NPs (Fig. 4a and 4b). Apart from some micellar aggregates attributed to the presence of unreacted precursor Fmoc-T,[24] the images also show that the nanofibers emanating from the NPs were long and clearly defined with a uniform diameter similar to previous studies (ca. 15 nm).[24-25] This indicated that the self-assembly proceeded from the NP surface in a process similar to regular free enzyme catalysis. In this scenario, the propagation of the self-assembled nanofibers from the enzyme-NP conjugates increases the masses and enlarges the NPs, retarding NP diffusion. Also, as fiber growth proceeded, the NP surface would become covered with nanofibers. Both these effects would slow the mass transport of precursors to the immobilized enzymes, thus resulting in the slowed and reduced conversion into Fmoc-TF-$NH_2$ observed in HPLC measurements.

2.3. Gelation Behavior of Chymotrypsin System 2

In the presence of free chymotrypsin, the precursors F-$NH_2$ and the dipeptide DF-OMe (*i.e.* aspartame) are known to form the tripeptide gelator DFF-$NH_2$, which self-assembles into a hydrogel composed of nanofibers. However, in a competing reaction, DFF-$NH_2$ is subsequently hydrolyzed also by chymotrypsin to give water soluble DF and F-$NH_2$. As a result of these competing processes, with formation kinetics that are faster than hydrolysis, a gel is rapidly but transiently formed and a gel-to-sol transition occurs in approximately 24 h under typical conditions.[25]

In the present study, an opaque dark brown gel is formed when we mixed the chymotrypsin-nanoparticle conjugates with the precursors DF-OMe (20 mM) and F-$NH_2$ (40 mM). This reaction proceeded within approximately 30 min, much quicker compared to the thermolysin System 1 (Fig. 4c, inset) but slower compared to the free chymotrypsin

enzyme system where gelation occurs within minutes. HPLC analysis confirmed that the conversion into the tripeptide gelator DFF-$NH_2$ was complete within approximately 6 h (Fig. 3a). The CD spectrum for System 2 shows a clear positive peak around 220 nm at t=5 min (Fig. 3b). Similar to System 1, this peak corresponds to the formation of chiral supramolecular arrangements as previously reported. [28]

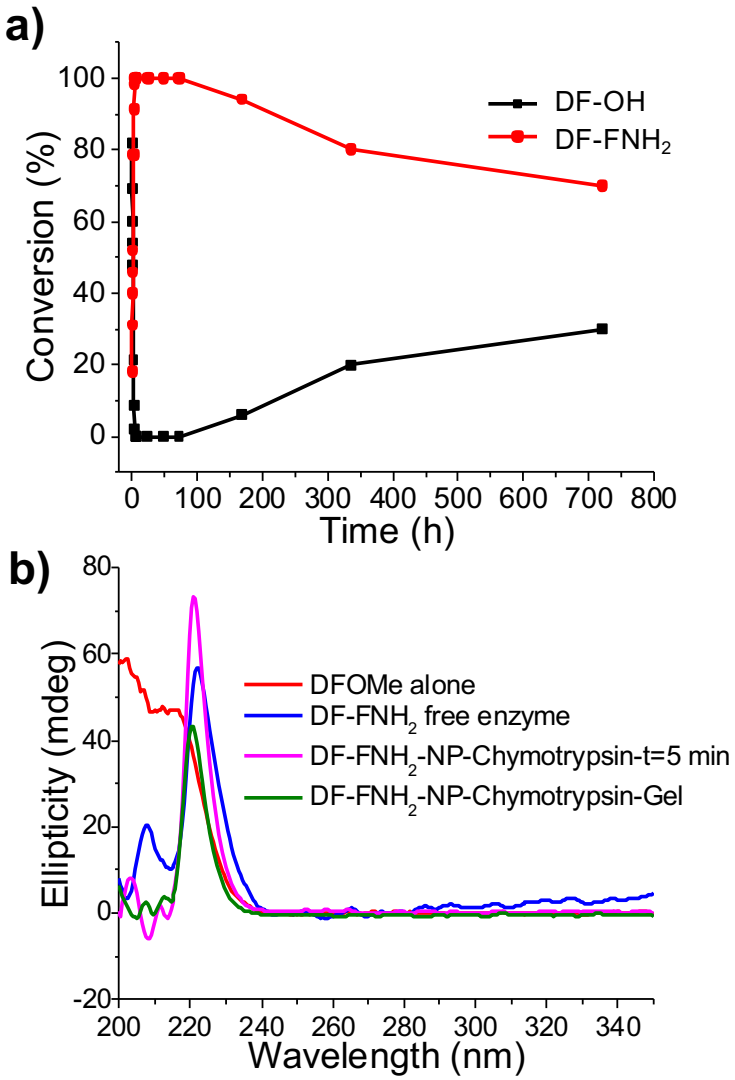

Figure 3: HPLC conversion (b) and CD spectra (c). For this System, the conversion into the tripeptide gelator DFF-$NH_2$ is complete within approximately 6 h. The observed CD spectrum shows a positive signal around 220 nm which suggests the formation of chiral supramolecular arrangements.

In contrast to previous studies with free chymotrypsin, the hydrogel formed with the chymotrypsin-NP conjugate remained stable for several months until the end of our study. Only HPLC analysis of the gel material was able to discern a slow hydrolysis, with the precursor conversion remaining at 80% after one month (Fig. 3a), much higher compared to that observed for the case of free chymotrypsin, where the percentage of conversion decreases to 10% after 72 h.[25] Thus, the lifetime of the hydrogel was dramatically enhanced by at least 30-fold, from 24 h to the end of HPLC studies at 1 month, by immobilizing the enzymes to the nanoparticles. This is related to the inability of the immobilized enzymes to freely diffuse toward the fibers for degradation, and therefore the nanofiber degradation kinetics was reduced.

TEM images of System 2, analogous to those of System 1, confirmed the formation of a network of nanofibers emanating from the surface of the nanoparticles (Fig. 4c and d). This meant that the enzyme-NP conjugates were trapped by interlocked fibers emanating from the NPs and could not freely diffuse. As a consequence, the NP-immobilized enzymes would only be able to act on the tripeptide self-assembly building blocks diffusing to or in immediate contact with them. However, all the tripeptides would have already been assembled into the nanofibers (*i.e.* sequestered) except for a minority exchanging with the solution phase. Thus, degradation of the self-assembled fibers would have been considerably retarded and the lifetime of the gel was significantly extended.

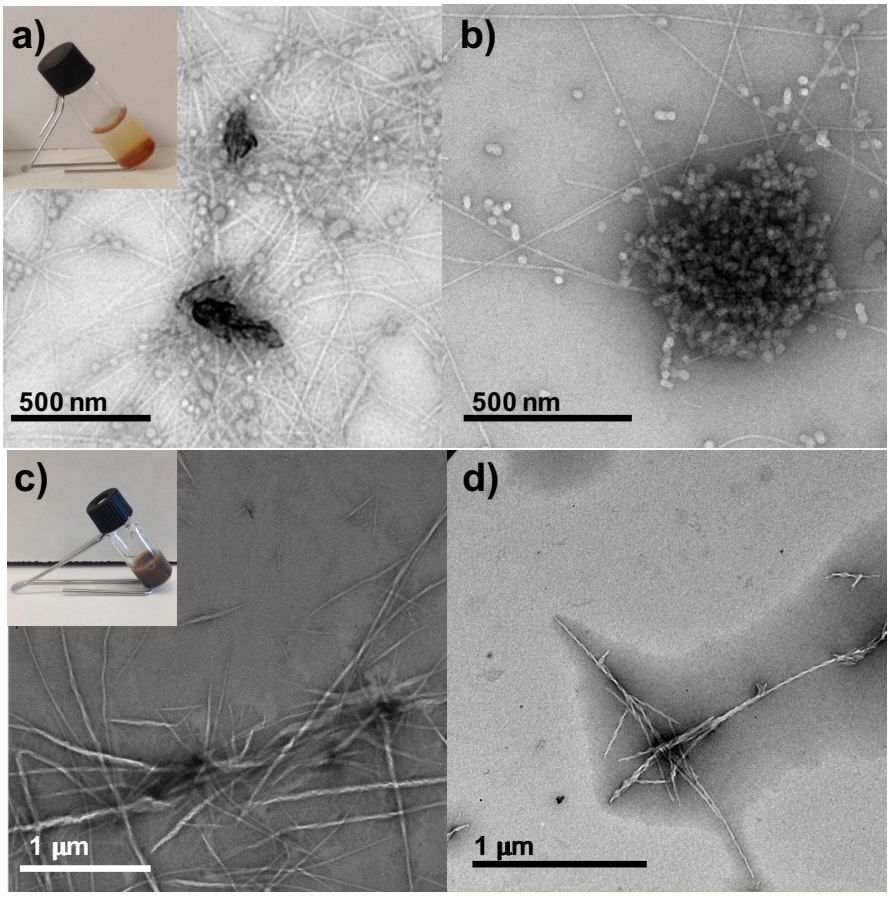


Figure 4: TEM images of the nanostructure formation catalyzed by the enzymes immobilized on the nanoparticles. For both System 1 (a and b) and System 2 (c and d), it is possible to observe the nucleation and growth of the nanofibers starting from the surface of the nanoparticles. In system 1 the spherical aggregates of excess Fmoc-T precursors are clearly visible. In the inset: digital images of the gels formed for System 1 (a) and System 2 (c).

## 2.4. Rheological Study of NP Connected Nanofibrous Hydrogel

As described in section 2.2, it is remarkable that the low precursor conversion observed in System 1 was still sufficient to form a bulk hydrogel. Moreover, TEM studies show nanofibrous networks connected by nanoparticle nodes (*i.e.* a hub-and-spoke morphology, Fig. 4 for both the thermolysin and chymotrypsin systems). With a modification of nanostructural arrangement usually comes a change in physical properties. Thus, we characterized the mechanical strength of the enzyme-NP catalyzed hydrogels.

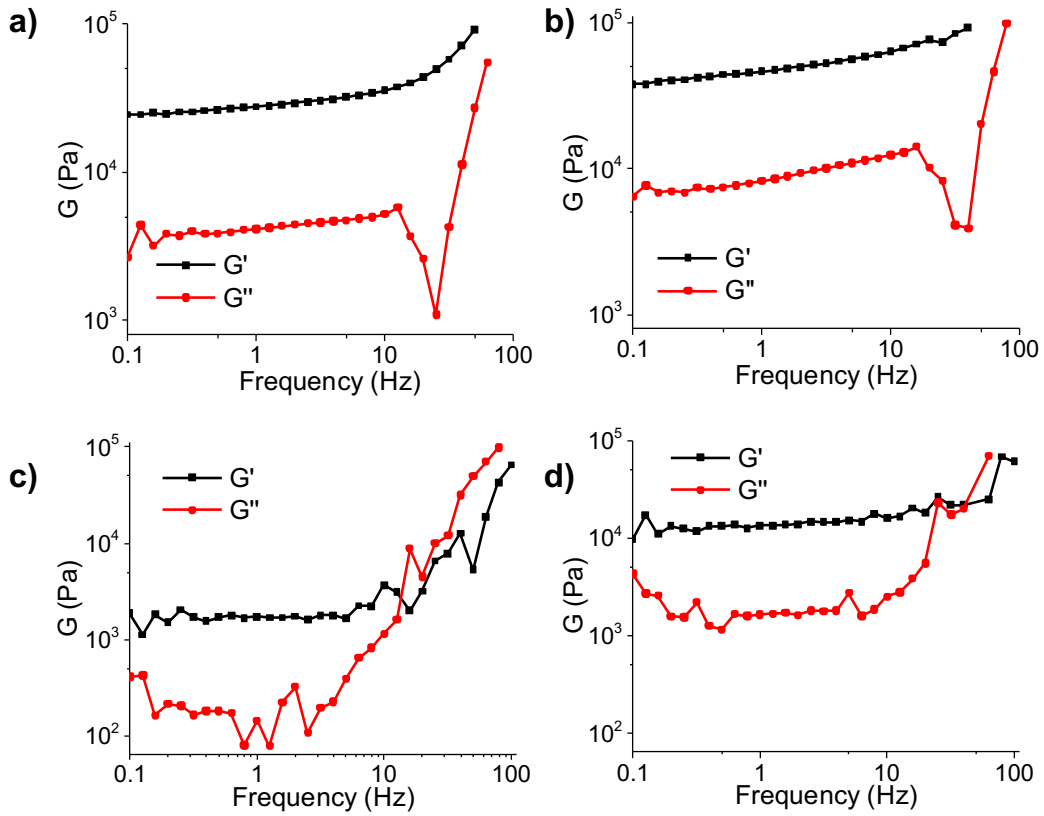


Figure 5: Dynamic frequency sweep experiments. a) FmocTF-$NH_2$ gels prepared with free thermolysin. G'= 35.5*$10^3$ Pa. b) Fmoc-TF-$NH_2$ gels prepared with thermolysin-nanoparticles conjugate. G'= 51.5*$10^3$ Pa. c) DFF-$NH_2$ gels prepared with free chymotrypsin. G'= 1.89*$10^3$ Pa. d) DFF-$NH_2$ gels prepared with the chymotrypsin-nanoparticles conjugates. G'= 15.42*$10^3$ Pa.

Strain controlled frequency sweep rheometry measurements were performed on both the thermolysin- and chymotrypsin-NP gels as well as on the corresponding gels formed with free enzymes, to characterize and compare the different types of structures (Fig. 5). For System 1, the use of the nanoparticle design resulted in a 44% increase of the storage modulus G', from 36 × $10^3$ Pa for the gel formed with free thermolysin to 52 × $10^3$ Pa for the gel formed with the enzyme-NP conjugates (values referring to the average in the

range between 0.1 and 10 Hz). However, even this modest increase in G' (and actually also in G'') is surprising because the conversion of the precursors to the self-assembling gelators was much lower in the nanoparticle system (6% vs. 81%[24]). This suggests that the NP-nanofiber hub-and-spoke morphology greatly enhanced the mechanical properties of a self-assembled hydrogel.

The effect of incorporating the nanoparticles is more dramatically evident in System 2, where G' increased by almost one order of magnitude, from $1.9 \times 10^3$ Pa for the gel obtained with free chymotrypsin to $15 \times 10^3$ Pa for the gel obtained with the enzyme-nanoparticle conjugates. Unlike System 1, high conversion of the precursors was obtained in System 2 using both the nanoparticle-mediated and free enzyme processes. We therefore attribute the large increase in mechanical strength to the immobilization of the enzyme on the nanoparticles and the resulting nanofiber arrangement around the NPs.

Saiani *et al*. also reported that a gel's mechanical strength could be improved by heterogeneous distribution of self-assembled nanofibers in a hydrogel, produced by solubilized enzymes that could generate gelators fast enough for immediate self-assembly before either the gelators or enzyme diffuse away.[29] In our system, the enzymes are immobilized on NPs that diffuse much slower than soluble molecules. Moreover, the large number of enzyme that can be immobilized on each NP acts to increase the local concentration of gelators formed. Therefore, localization of self-assembly and any enhancement in properties is less limited to systems with fast kinetics (*e.g*. System 1).

### 2.5. External Manipulation of Hydrogel System

The magnetic nature of our enzyme-nanoparticle conjugates offered a convenient way to manipulate our nanoparticle-linked system. Given the long time required for System 1 to gel, we focused on the chymotrypsin System 2. In a first set of experiments to test the basic response to an externally applied magnetic field, 100 $\mu$l of the mixture of precursors and chymotrypsin-NP conjugates was placed in a well of a 96-well cell culture plate, and a small permanent magnet was introduced in the vicinity of the mixture, immediately after mixing the components. We tested the magnet placement in three different positions (Fig. S4): on top of the well (Position 1), and 1.2 cm and 2.4 cm from the side of the well (Positions 2 and 3, respectively). The system was then left to equilibrate.

When the magnet was placed in Position 1, the nanoparticles immediately migrated to the top of the solution, "switching off" the gelation process (Fig. S4a). When the magnet was placed in Position 2, formation of a gel with a gradation of color was observed overnight (Fig. S4b). When the magnet was in position 3, no effect on the gel appearance was observed (Fig. S4c), but the gelation occurred slower compared to the case when no magnet was introduced (3 to 4 h compared to 30 min), suggesting that the nanoparticles were displaced by the magnet to some extent.

The color gradation of the gel could indicate a gradient in the density of self-assembled nanofibers across the gel, resulting from the slow migration of the nanoparticles towards the magnet. Such a variation in nanofiber density could presumably correspond to a gradient in mechanical properties. However, local mechanical characterization of a soft hydrogel is challenging and is beyond the scope of the present study.

In a second experiment, to investigate the effect of a magnetic field after the gel has formed, the magnet was placed next to a vial containing an already formed gel (Fig. 6).

This gel was observed to slowly shrink over time, approximately by half after 1 weak, and finally reaching approximately 15% of its original volume after one month. The change in the gel volume after 1 month was permanent, since if the magnet is removed, the gel does not relax to its original shape. HPLC analysis showed a much lower concentration of DFF-$NH_2$ in the transparent supernatant outside the gel (conversion of less than 20%) than in the contracted gel part of the system (conversion remaining as high as 70% after 1 month; see section 9 in ESI). This difference in DFF-$NH_2$ content is consistent with the TEM characterization that shows very few fibers in the supernatant, but a high density of fibers in the contracted gel (Fig. 6).

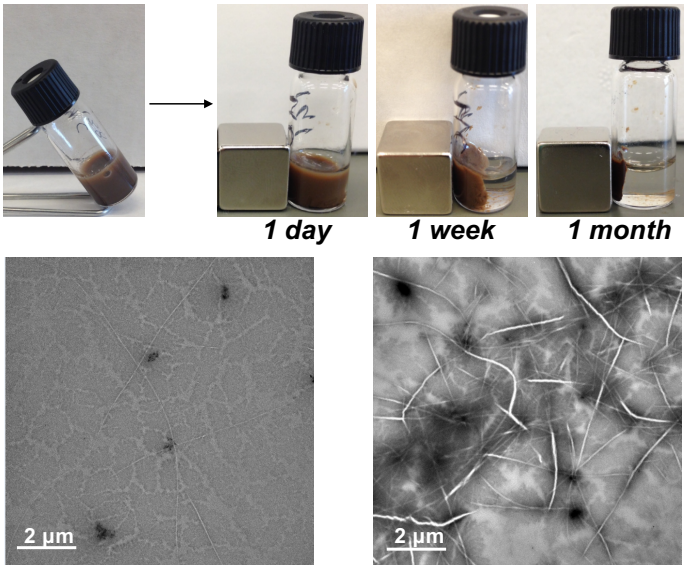


Figure 6: (a) Images to show the effect of a magnetic field on the DF-$FNH_2$ gel formed with the chymotrypsin-nanoparticles. The gel progressively shrinks over time under the effect of the magnetic field reaching approximately 15% of its initial volume after 1 month. TEM images of transparent supernatant collected upon separation with the magnetic cube (b) and of the compacted gel (c).

This second experiment shows that the gel may be separated together with the nanoparticle conjugates, even when the strength of the nanofibrous network and the

osmotic pressure associated with "squeezing out" the supernatant acting against the NPs. This implies that the self-assembled nanofibres were strongly associated with the NP surface, as also suggested by the significant enhancement of mechanical properties for the NP-mediated hydrogels (Fig.5), even if they were formed from a relatively low precursor conversion (Fig.2). The integration of the nanofibers and NPs consequently provides a means to externally manipulate the system with an applied magnetic field.

In fact, a strong association of the nanofibers with the NPs as well as the relatively slow precursor conversion kinetics observed (see sections 2.2 and 2.3) are both expected, if gelator production and nanofiber self-assembly were localized on the enzyme-NP surfaces such that a concentration of nanofibers could adhere around the NPs. This was indeed observed in TEM (Fig.4). The possibility to closely specify the location of self-assembly was also suggested by our previous observation of nanofiber networks on enzyme-functionalized flat surfaces.[23] Thus the overall experimental evidence supports the hypothesis that surface-immobilized enzymes could direct nucleation and self-assembly of nanostructures.

## 3. Conclusion

We demonstrated the use of enzymes immobilized on magnetic nanoparticles for both an equilibrium and a non-equilibrium biocatalytic self-assembling peptide hydrogel systems. By simply immobilizing the biocatalyst on NPs and hence localizing the initiation of nanofiber self-assembly, we could change the hydrogel nanostructural organization from a random arrangement to an overall "hub-and-spoke" morphology where the nanofibers can be linked through the enzyme-NP conjugates. This resulted,

depending on the system, in a 2 to 10-fold enhancement of the mechanical modulus of the hydrogel compared to a conventional soluble enzyme system. We hypothesize that the NPs may act as nodes of concentrated nanofibers that help in joining together the fibrous network. Localization of the enzyme also dramatically restricted the enzyme's ability to mediate degradation side reactions that would otherwise have dissipated the nanofibers, and thus enabled unprecedented control (a >30-fold extension) in the lifetime of a self-assembled hydrogel.

In addition, we demonstrated magnetic manipulation of the self-assembly system. Application of an external magnetic field enabled "switching off" of self-assembly. Application post-gelation could pull the NPs along with their associated nanofibers, resulting in a more than 6-fold compaction in the hydrogel volume. If functional groups were incorporated into the nanofibers, behaviors that depend on chemical concentrations may also be enabled. The expulsion of the sol phase is also essentially a mechanism for material release.

In summary, immobilizing the (bio)catalyst on magnetic nanoparticles and hence localizing the nucleation of (bio)catalytic nanofiber self-assembly, it is possible not only to enhance the mechanical properties of a nanofibrous hydrogel network, but also to control the timing of its formation, its lifetime, as well as to confer stimuli-responsiveness to the self-assembled nanostructure.

## ASSOCIATED CONTENT

**Supporting Information:** Details on experimental procedures and sample characterization

AUTHOR INFORMATION

**Corresponding Author**

*E-mail: aaron.lau@strath.ac.uk

*E-mail: rein.ulijn@asrc.cuny.edu

**Author Contributions**

The manuscript was written through contributions of all authors. All authors have given approval to the final version of the manuscript.

ACKNOWLEDGMENT

The authors gratefully acknowledge the financial support by the EC 7th Framework Programme Marie Curie Actions via the European ITN SMARTNET No. 316656. This material is based upon work supported by, or in part by, the U. S. Army Research Laboratory and the U. S. Army Research office under contract/grant number W911NF-16-1-0113. They also acknowledge Margaret Mullin from University of Glasgow and Tong Wang from the ARSC in CUNY for their help in TEM imaging.

REFERENCES

1. Hartgerink, J. D.; Beniash, E.; Stupp, S. I., Self-Assembly and Mineralization of Peptide-Amphiphile Nanofibers. *Science* **2001,** *294* (5547), 1684-1688.

2. Whitesides, G. M.; Grzybowski, B., Self-Assembly at All Scales. *Science* **2002,** *295* (5564), 2418-21.

3. Lehn, J.-M., Toward Self-Organization and Complex Matter. *Science* **2002,** *295* (5564), 2400-2403.

4. Mattia, E.; Otto, S., Supramolecular Systems Chemistry. *Nat. Nano.* **2015,** *10* (2), 111-119.

5. Yang, Z.; Liang, G.; Xu, B., Enzymatic Hydrogelation of Small Molecules. *Acc. Chem. Res.* **2008,** *41* (2), 315-326.

6. Cui, H.; Webber, M. J.; Stupp, S. I., Self-Assembly of Peptide Amphiphiles: From Molecules to Nanostructures to Biomaterials. *J. Pept. Sci.* **2010,** *94* (1), 1-18.

7. Liu, Y.; Terrell, J. L.; Tsao, C.-Y.; Wu, H.-C.; Javvaji, V.; Kim, E.; Cheng, Y.; Wang, Y.; Ulijn, R. V.; Raghavan, S. R.; Rubloff, G. W.; Bentley, W. E.; Payne, G. F., Biofabricating Multifunctional Soft Matter with Enzymes and Stimuli-Responsive Materials. *Adv. Funct. Mater.* **2012,** *22* (14), 3004-3012.

8. Fichman, G.; Gazit, E., Self-Assembly of Short Peptides to Form Hydrogels: Design of Building Blocks, Physical Properties and Technological Applications. *Acta Biomater.* **2014,** *10* (4), 1671-1682.

9. Webber, M. J.; Appel, E. A.; Meijer, E. W.; Langer, R., Supramolecular Biomaterials. *Nat. Mater.* **2016,** *15* (1), 13-26.

10. Zhou, J.; Li, J.; Du, X.; Xu, B., Supramolecular Biofunctional Materials. *Biomaterials* **2017,** *129*, 1-27.

11. Hirst, A. R.; Escuder, B.; Miravet, J. F.; Smith, D. K., High-Tech Applications of Self-Assembling Supramolecular Nanostructured Gel-Phase Materials: From Regenerative Medicine to Electronic Devices. *Angew. Chem. Int. Ed.* **2008,** *47* (42), 8002-8018.

12. Hirst, A. R.; Roy, S.; Arora, M.; Das, A. K.; Hodson, N.; Murray, P.; Marshall, S.; Javid, N.; Sefcik, J.; Boekhoven, J.; van Esch, J. H.; Santabarbara, S.; Hunt, N. T.; Ulijn, R. V., Biocatalytic Induction of Supramolecular Order. *Nat. Chem.* **2010,** *2* (12), 1089-94.

13. Olive, A. G. L.; Abdullah, N. H.; Ziemecka, I.; Mendes, E.; Eelkema, R.; van Esch, J. H., Spatial and Directional Control over Self-Assembly Using Catalytic Micropatterned Surfaces. *Angew. Chem. Int. Ed.* **2014,** *126* (16), 4216-4220.

14. Yang, Z.; Gu, H.; Fu, D.; Gao, P.; Lam, J. K.; Xu, B., Enzymatic Formation of Supramolecular Hydrogels. *Adv. Mater.* **2004,** *16* (16), 1440-1444.

15. Debnath, S.; Roy, S.; Ulijn, R. V., Peptide Nanofibers with Dynamic Instability through Nonequilibrium Biocatalytic Assembly. *J. Am. Chem. Soc.* **2013,** *135* (45), 16789-16792.

16. Williams, R. J.; Smith, A. M.; Collins, R.; Hodson, N.; Das, A. K.; Ulijn, R. V., Enzyme-Assisted Self-Assembly under Thermodynamic Control. *Nat. Nanotechnol.* **2009,** *4* (1), 19-24.

17. Vigier-Carrière, C.; Garnier, T.; Wagner, D.; Lavalle, P.; Rabineau, M.; Hemmerlé, J.; Senger, B.; Schaaf, P.; Boulmedais, F.; Jierry, L., Bioactive Seed Layer for Surface-Confined Self-Assembly of Peptides. *Angew. Chem. Int. Ed.* **2015,** *54* (35), 10198-10201.

18. Vigier-Carrière, C.; Wagner, D.; Chaumont, A.; Durr, B.; Lupattelli, P.; Lambour, C.; Schmutz, M.; Hemmerlé, J.; Senger, B.; Schaaf, P.; Boulmedais, F.; Jierry, L., Control of Surface-Localized, Enzyme-Assisted Self-Assembly of Peptides through Catalyzed Oligomerization. *Langmuir* **2017,** *33* (33), 8267-8276.

19. Yang, Z. M.; Xu, K. M.; Guo, Z. F.; Guo, Z. H.; Xu, B., Intracellular Enzymatic Formation of Nanofibers Results in Hydrogelation and Regulated Cell Death. *Adv. Mater.* **2007,** *19* (20), 3152-3156.

20. Kuang, Y.; Shi, J.; Li, J.; Yuan, D.; Alberti, K. A.; Xu, Q.; Xu, B., Pericellular Hydrogel/Nanonets Inhibit Cancer Cells. *Angew. Chem. Int. Ed.* **2014,** *53* (31), 8104-8107.

21. Pires, R. A.; Abul-Haija, Y. M.; Costa, D. S.; Novoa-Carballal, R.; Reis, R. L.; Ulijn, R. V.; Pashkuleva, I., Controlling Cancer Cell Fate Using Localized Biocatalytic Self-Assembly of an Aromatic Carbohydrate Amphiphile. *J. Am. Chem. Soc.* **2015,** *137* (2), 576-579.

22. Fabijanic, K. I.; Perez-Castillejos, R.; Matsui, H., Direct Enzyme Patterning with Microcontact Printing and the Growth of Zno Nanoparticles on the Catalytic Templates at Room Temperature. *J. Mater. Chem.* **2011,** *21* (42), 16877.

23. Conte, M. P.; Lau, K. H. A.; Ulijn, R. V., Biocatalytic Self-Assembly Using Reversible and Irreversible Enzyme Immobilization. *ACS Appl. Mater. Interfaces* **2017,** *9* (4), 3266-3271.

24. Sasselli, I. R.; Pappas, C. G.; Matthews, E.; Wang, T.; Hunt, N. T.; Ulijn, R. V.; Tuttle, T., Using Experimental and Computational Energy Equilibration to Understand Hierarchical Self-Assembly of Fmoc-Dipeptide Amphiphiles. *Soft Matter* **2016**.

25. Pappas, C. G.; Sasselli, I. R.; Ulijn, R. V., Biocatalytic Pathway Selection in Transient Tripeptide Nanostructures. *Angew. Chem. Int. Ed.* **2015,** *54* (28), 8119-8123.

26. Beljonne, D.; Curutchet, C.; Scholes, G. D.; Silbey, R. J., Beyond Förster Resonance Energy Transfer in Biological and Nanoscale Systems. *J. Phys. Chem. B* **2009,** *113* (19), 6583-6599.

27. Cheng, G.; Castelletto, V.; Moulton, C. M.; Newby, G. E.; Hamley, I. W., Hydrogelation and Self-Assembly of Fmoc-Tripeptides: Unexpected Influence of Sequence on Self-Assembled Fibril Structure, and Hydrogel Modulus and Anisotropy. *Langmuir* **2010,** *26* (7), 4990-4998.

28. Marchesan, S.; Waddington, L.; Easton, C. D.; Winkler, D. A.; Goodall, L.; Forsythe, J.; Hartley, P. G., Unzipping the Role of Chirality in Nanoscale Self-Assembly of Tripeptide Hydrogels. *Nanoscale* **2012,** *4* (21), 6752-6760.

29. Guilbaud, J.-B.; Rochas, C.; Miller, A. F.; Saiani, A., Effect of Enzyme Concentration of the Morphology and Properties of Enzymatically Triggered Peptide Hydrogels. *Biomacromolecules* **2013,** *14* (5), 1403-1411.